Structural Engineering and Mechanics, *Vol. 57, No. 1 (2016) 65-89*
DOI: http://dx.doi.org/10.12989/sem.2016.57.1.065

XFEM for fatigue and fracture analysis of cracked stiffened panels

M.R. Nanda Kumar[1a], A. Ramachandra Murthy[*2], Smitha Gopinath[2b] and Nagesh R. Iyer[2c]

[1]*Bhabha Atomic Research Centre, Mumbai, 400085, India*
[2]*CSIR-Structural Engineering Research Centre, Chennai, 600113, India*

(Received November 19, 2014, Revised December 1, 2015, Accepted December 2, 2015)

Abstract. This paper presents the development of methodologies using Extended Finite Element Method (XFEM) for cracked unstiffened and concentric stiffened panels subjected to constant amplitude tensile fatigue loading. XFEM formulations such as level set representation of crack, element stiffness matrix formulation and numerical integration are presented and implemented in MATLAB software. Stiffeners of the stiffened panels are modelled using truss elements such that nodes of the panel and nodes of the stiffener coincide. Stress Intensity Factor (SIF) is computed from the solutions of XFEM using domain form of interaction integral. Paris's crack growth law is used to compute the number of fatigue cycles up to failure. Numerical investigations are carried out to model the crack growth, estimate the remaining life and generate damage tolerant curves. From the studies, it is observed that (i) there is a considerable increase in fatigue life of stiffened panels compared to unstiffened panels and (ii) as the external applied stress is decreasing number of fatigue life cycles taken by the component is increasing.

Keywords: extended finite element method; fatigue; stress intensity factor; stiffened panels

1. Introduction

Many real life structural components such as aerospace structural components, ship hull structures, off shore structural components are subjected to fatigue loading. These components contain internal defects such as cracks, inclusions, voids which are developed during manufacturing stage or at service stage. Structural panels are stiffened with stiffeners which improve the strength and stiffness of the panels, strength to weight ratio, vibration and buckling properties depending on the size and position of the stiffeners. Stiffeners act as crack arrestors which retard the crack growth and increase the number of loading cycles. The prediction of number of cycles of loading required to grow a crack to a certain length is very important in the assessment of service durability and structural life prediction which helps in determining the

∗Corresponding author, Scientist, E-mail: murthyarc@serc.res.in
[a]Trainee Scientific Officer
[b]Scientist
[c]Former Director

http://www.techno-press.org/?journal=sem&subpage=8 ISSN: 1225-4568 (Print), 1598-6217 (Online)

proper inspection intervals which could prevent the catastrophic failure.

Stress Intensity Factor is an influential fracture parameter which needs to be evaluated in order to carry out damage tolerant analysis. There are hand books (Murakami 1986, Rooke *et al*. 1976) available for the computation of SIF for simple crack geometry and loading. But for complicated crack geometry and loading, inevitably one has to go for numerical techniques. Hence a stable numerical method is required to model the structural panel, stiffeners, crack and crack growth with low computational effort and good accuracy. In this paper XFEM is used as a numerical tool to carry out damage tolerant analysis of cracked unstiffened and concentric stiffened panels subjected to tensile fatigue loading.

Hence a stable numerical method is required to model the structural panel, crack and crack growth with low computational cost and good accuracy. Modelling of moving discontinuities (cracks) in finite element framework is a difficult task because of the need to update the mesh at each step as the crack propagates. A very fine mesh is required near the vicinity of the crack and mesh need to be conforming to the sides of the crack. Also the singularity at the crack tip must be accurately represented (Tong *et al*.1973) Another way of handling discontinuities such as cracks is to model the crack which is independent of the mesh. XFEM is one of the advanced numerical methods for fracture analysis of structural components. In this paper XFEM has been used as a numerical tool to carry out fracture analysis and estimate remaining life.

XFEM can be used to add discontinuous enrichment functions to the original finite element approximation (Belytschko *et al*.1999, Moes *et al*. 1999 and Dolbow *et al*. 2000) through the partition of unity (Melenk and Babuska 1996). In XFEM, a standard finite element mesh is created without accounting for the geometric entity. The presence of discontinuity is then represented independently of the mesh by enriching the standard displacement based approximation with additional functions. For crack modelling, both discontinuous displacement fields (Heaviside step function) along the crack faces and leading singular asymptotic crack tip displacement fields are added to the displacement based standard finite element approximation through partition of unity. In addition, XFEM provides a seamless means to use higher order elements or special FEs without significant changes in the formulation. The XFEM will also improve the accuracy in problems where some aspects of the functional behaviour of the solution field is known a priori and relevant enrichment functions can then be used.

Jiang *et al.* (2014) implemented the XFEM program to investigate the effects of voids, inclusions and minor cracks on the path of major crack propagation. Omidi *et al* (2014) applied XFEM methodologies to examine the fracture behaviour of centrally cracked aluminium plates with single and double sided composite patches. XFEM was applied by Natarajan *et al.* (2014) to study the inclusion and crack interaction in an elastic medium. Both the crack and inclusions were modelled in XFEM frame work. Sharma *et al.* (2014) studied the effect of inhomogeneities such as cracks, inclusions and voids on the stress intensity factor using XFEM. Meng *et al* .(2014) implemented XFEM to model the crack growth in the power law creep materials. XFEM was used by Rasuo *et al*. (2013) for fatigue life investigation of 2024-T3 aluminium spar of light aircraft. Both experimental and numerical analysis have been carried out where FEM has been used for estimation of spar life to crack initiation, whereas XFEM has been used for fatigue crack growth predictions. Himanshu *et al*.(2013) simulated the 3-D fatigue crack growth problem in XFEM. Singh *et al*. (2012) used the XFEM to simulate the fatigue crack growth of panels with multiple discontinuities.

Dorata *et al.* (2012) presented a probabilistic method to predict fatigue crack growth and fatigue life of structural components subjected to variable amplitude loading. Ramachandra

Murthty *et al*. (2009a 2009b, 2007) developed methodologies for remaining life prediction of cracked stiffened panels under constant and variable amplitude loading. Sabelkin *et al*. (2006) has conducted experimental and analytical investigations to study the fatigue crack growth behaviour of stiffened 20124-T3 aluminium panels repaired with one sided adhesively bonded composite patch. Nechval *et al.* (2006) developed an artificial neural network model for the prediction of fatigue crack growth of cracked structural components. Dexter *et al*. (2005, 2003) developed a long fatigue crack growth model of stiffened panels and compared the model with the finite element analysis. Though lot of research has been done in the development of XFEM in recent past, implementation of XFEM need to be verified before it can be applied to large scale practical problems. To the best of authors knowledge there is no work reported till date using XFEM to model the cracked stiffened panels and to predict the fatigue life of stiffened structural components.

In this paper, both cracked stiffened and unstiffened structural panels have been subjected to constant amplitude tensile fatigue loading. The stress intensity factors have been evaluated from the XFEM solution to estimate the fatigue life of stiffened and unstiffened 350WT steel cracked panel subjected to constant amplitude tensile fatigue loading. Crack has been modelled as a linear combination of line segments using level set representation. Stiffeners have been modelled as truss elements such that nodes of the panels and nodes of the stiffeners coincide. Maximum hoop stress criterion has been used to find the direction of crack propagation. The stress intensity factors have been computed using domain form of interaction integral approach. Paris crack growth law has been used to model the fatigue life of 350WT steel panels. The studies made in this paper may be useful for damage tolerant design of structural components.

2. XFEM formulations

In XFEM, the following approximation is used to compute the displacement for the point **x** located within the domain (Belytschko *et al*. 1999)

$$\mathbf{u}^{h}(\mathbf{x}) = \mathbf{u}^{FE} + \mathbf{u}^{enr} = \sum_{i=1}^{n} N_i(\mathbf{x})\mathbf{u_i} + \sum_{k=1}^{m} N_k(\mathbf{x})\psi(\mathbf{x})\mathbf{a_k} \tag{1}$$

where $\mathbf{u}_i$ is the vector of regular degrees of nodal freedom in the finite element method, n is the total number of nodes in finite element model, N_i shape function associated with node i, $\mathbf{a}_k$ is the added set of degrees of freedom to the standard finite element model, m is the number of enriched nodes and $\psi(\mathbf{x})$ is the discontinuous enrichment function defined for the set of nodes that the discontinuity has in its influence (support) domain. The enrichment function $\psi(\mathbf{x})$ can be chosen by applying appropriate analytical solutions according to the type of discontinuity. The first term on the right hand side of Eq. (1) is the classical finite element approximation to determine the displacement field, while the second term is the enrichment approximation which takes into account the existence of any discontinuities. The second term utilises additional degrees of freedom to facilitate modelling the existence of any discontinuous field, such as a crack, without modelling it explicitly in the finite element mesh.

When XFEM is applied to fracture mechanics problems, displacement field is taken as (Moes *et al* 1999)

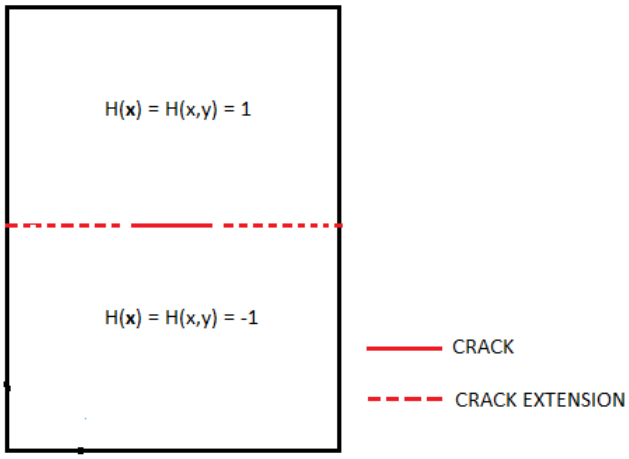

Fig. 1 Heaviside enrichment function definition

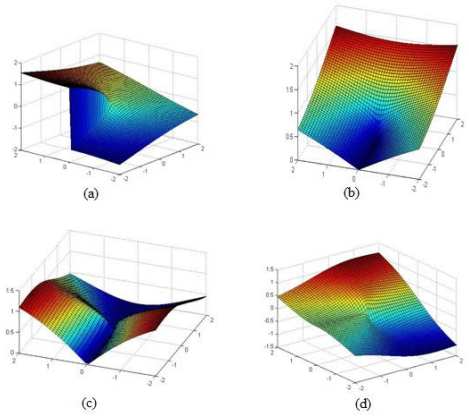

Fig. 2 Crack tip enrichment functions F_l, l=1,2,3,4 (a) F_1, (b) F_2, (c) F_3, (d) F_4

$$\mathbf{u}^{h}(\mathbf{x}) = \sum_{i=1}^{n} N_i(\mathbf{x})\mathbf{u_i} + \sum_{j\in J} N_j(\mathbf{x})H(\mathbf{x})\mathbf{a_j} + \sum_{k\in K_1} N_k\left(\sum_{l=1}^{4} F_l^1(\mathbf{x})\mathbf{b_{kl}^1}\right) + \sum_{k\in K_2} N_k\left(\sum_{l=1}^{4} F_l^2(\mathbf{x})\mathbf{b_{kl}^2}\right) \quad (2)$$

where, H(**x**) is the heaviside enrichment function defined such that it equals 1 for all **x** above the crack and -1 for all **x** below the crack as shown in the Fig. 1 and $\mathbf{a_j}$ is the heaviside enriched node. J is the set of nodes, enriched with heaviside enrichment function, whose nodal shape function support contain crack but not crack tip.

Here k_1 and k_2 are the set of nodes, associated with crack tips 1 and 2, whose element contain crack tips respectively; $\mathbf{b}_{kl}^1$, $\mathbf{b}_{kl}^2$, are vectors of additional degrees of nodal freedom for modelling crack faces and the two crack tips. The crack tip enrichment function is given by $F_l(\mathbf{x})$ which is given as

$$F_l(r,\theta)_{l=1}^4 = \left[\sqrt{r}\sin\frac{\theta}{2}, \sqrt{r}\cos\frac{\theta}{2}, \sqrt{r}\sin\theta\sin\frac{\theta}{2}, \sqrt{r}\sin\theta\cos\frac{\theta}{2}\right] \quad (3)$$

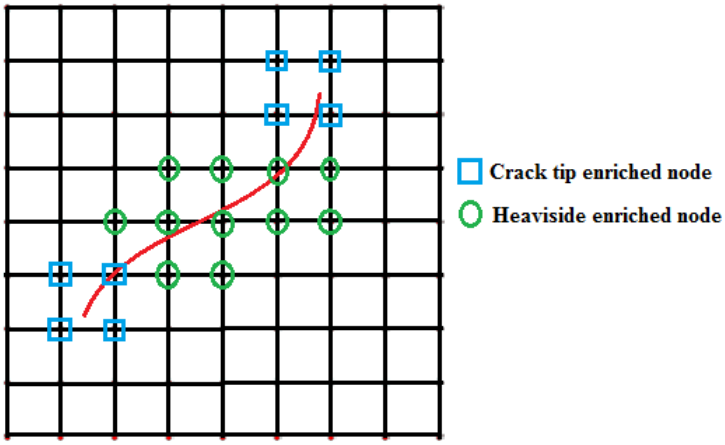

Fig. 3 Nodal enrichment strategy

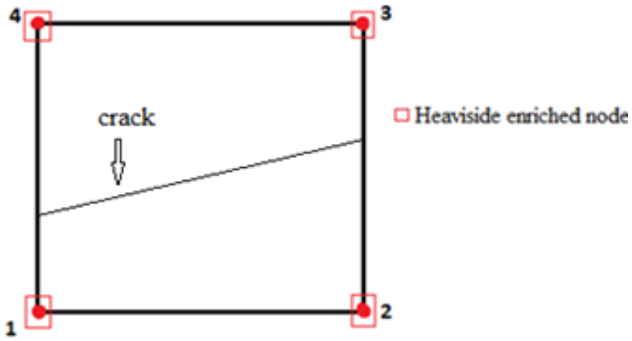

Fig. 4 Fully heaviside enriched element

where (r,θ) are crack tip polar coordinate system. The graphical representation of Eq. (3) is shown in Fig. 2.

From the Fig. 2 it is clear that F_1 is discontinuous function and rest of the functions are continuous. Thus F_1 models the discontinuity from the tip of the crack to the edge of the crack tip enriched element. Nodal enrichment strategy is shown in Fig. 3.

When a classical finite element node is enriched with heaviside enrichment we get additionally two unknown coefficients and with crack tip enrichment function eight unknown coefficients.

2.1 Element stiffness matrix formulation

Elements in XFEM can be classified into four types where first type is fully enriched elements with crack tip enrichment, second is fully enriched element with Heaviside enrichment, third is partially enriched element, fourth is classical standard finite element with no enrichment. In this section the element stiffness matrix formulations of fully enriched element with Heaviside enrichment and crack tip enrichment are presented. Subsequently, a generalized formulation has been presented. First consider the element stiffness matrix formulation for fully enriched element with Heaviside enrichment as shown in Fig. 4.

The displacement field is calculated as

$$u = N_1 u_1 + N_2 u_2 + N_3 u_3 + N_4 u_4 + N_1 H a_1 + N_2 H a_2 + N_3 H a_3 + N_4 H a_4 \tag{4}$$

$$v = N_1 v_1 + N_2 v_2 + N_3 v_3 + N_4 v_4 + N_1 H b_1 + N_2 H b_2 + N_3 H b_3 + N_4 H b_4 \tag{5}$$

Writing the above equations in matrix form

$$\mathbf{u^h(x)} = \begin{bmatrix} \mathbf{N_{fem}} & \mathbf{N_{enr}} \end{bmatrix} \begin{Bmatrix} \mathbf{u} \\ \mathbf{a} \end{Bmatrix} \tag{6}$$

where

$$\mathbf{u^h(x)} = \begin{Bmatrix} u \\ v \end{Bmatrix} \tag{7}$$

$$\mathbf{N_{fem}} = \begin{bmatrix} N_1 & 0 & N_2 & 0 & N_3 & 0 & N_4 & 0 \\ 0 & N_1 & 0 & N_2 & 0 & N_3 & 0 & N_4 \end{bmatrix} \tag{8}$$

$$\mathbf{N_{enr}} = \begin{bmatrix} N_1 H & 0 & N_2 H & 0 & N_3 H & 0 & N_4 H & 0 \\ 0 & N_1 H & 0 & N_2 H & 0 & N_3 H & 0 & N_4 H \end{bmatrix} \tag{9}$$

$\mathbf{N_{fem}}$, $\mathbf{N_{enr}}$ are finite element shape functions and enriched element shape functions respectively and **u**, **a** are classical finite element degrees of freedom and enriched element degrees of freedom respectively.

$$\mathbf{u} = \begin{Bmatrix} u_1 \\ v_1 \\ u_2 \\ v_2 \\ u_3 \\ v_3 \\ u_4 \\ v_4 \end{Bmatrix} \mathbf{a} = \begin{Bmatrix} a_1 \\ b_1 \\ a_2 \\ b_2 \\ a_3 \\ b_3 \\ a_4 \\ b_4 \end{Bmatrix} \tag{10}$$

Thus displacement field in XFEM context is written as

$$\mathbf{u^h(x)} = \mathbf{N_{fem}u} + \mathbf{N_{enr}a} \tag{11}$$

Assuming small displacement and small strain theory

$$\varepsilon_x = \frac{\partial u}{\partial x} \quad \varepsilon_y = \frac{\partial v}{\partial y} \quad \gamma_{xy} = \frac{\partial u}{\partial y} + \frac{\partial v}{\partial x} \tag{12}$$

Writing in matrix form leads to

$$\boldsymbol{\varepsilon} = \begin{bmatrix} \mathbf{B_{fem}} & \mathbf{B_{enr}} \end{bmatrix} \begin{Bmatrix} \mathbf{u} \\ \mathbf{a} \end{Bmatrix} \tag{13}$$

where

$$\boldsymbol{\varepsilon} = \begin{Bmatrix} \varepsilon_x \\ \varepsilon_y \\ \gamma_{xy} \end{Bmatrix} \tag{14}$$

$$\mathbf{B}_{\mathbf{fem}} = \begin{bmatrix} N_{1,x} & 0 & N_{2,x} & 0 & N_{3,x} & 0 & N_{4,x} & 0 \\ 0 & N_{1,y} & 0 & N_{2,y} & 0 & N_{3,y} & 0 & N_{4,y} \\ N_{1,y} & N_{1,x} & N_{2,y} & N_{2,x} & N_{3,y} & N_{3,x} & N_{4,y} & N_{4,x} \end{bmatrix} \tag{15}$$

$$\mathbf{B}_{\mathbf{enr}} = \begin{bmatrix} (N_1H)_{,x} & 0 & (N_2H)_{,x} & 0 & (N_3H)_{,x} & 0 & (N_4H)_{,x} & 0 \\ 0 & (N_1H)_{,y} & 0 & (N_2H)_{,y} & 0 & (N_3H)_{,y} & 0 & (N_4H)_{,y} \\ (N_1H)_{,y} & (N_1H)_{,x} & (N_2H)_{,y} & (N_2H)_{,x} & (N_3H)_{,y} & (N_3H)_{,x} & (N_4H)_{,y} & (N_4H)_{,x} \end{bmatrix} \tag{16}$$

From theory of elasticity, the strain energy stored in a body is given by

$$U = \frac{1}{2}\int_{\Omega} \boldsymbol{\sigma}^{\mathbf{T}} \boldsymbol{\varepsilon} d\Omega \tag{17}$$

But, $\boldsymbol{\sigma}=\mathbf{D}\boldsymbol{\varepsilon}$, where $\mathbf{D}$ is the elasticity matrix. Thus

$$U = \frac{1}{2}\int_{\Omega} \boldsymbol{\varepsilon}^{\mathbf{T}} \mathbf{D} \boldsymbol{\varepsilon} d\Omega \tag{18}$$

Substituting Eq. (13) into (18),

$$U = \frac{1}{2}\int_{\Omega} \left((\mathbf{B}_{\mathbf{fem}}\mathbf{u})^{\mathbf{T}} + (\mathbf{B}_{\mathbf{enr}}\mathbf{a})^{\mathbf{T}} \right) (\mathbf{D}\mathbf{B}_{\mathbf{fem}}\mathbf{u} + \mathbf{D}\mathbf{B}_{\mathbf{enr}}\mathbf{a}) d\Omega \tag{19}$$

$$U = \frac{1}{2}\mathbf{u}^{\mathbf{T}} \left\{ \int_{\Omega} \mathbf{B}_{\mathbf{fem}}^{\mathbf{T}} \mathbf{D}\mathbf{B}_{\mathbf{fem}} d\Omega \right\} \mathbf{u} + \frac{1}{2}\mathbf{u}^{\mathbf{T}} \left\{ \int_{\Omega} \mathbf{B}_{\mathbf{fem}}^{\mathbf{T}} \mathbf{D}\mathbf{B}_{\mathbf{enr}} d\Omega \right\} \mathbf{a} + \frac{1}{2}\mathbf{a}^{\mathbf{T}} \left\{ \int_{\Omega} \mathbf{B}_{\mathbf{enr}}^{\mathbf{T}} \mathbf{D}\mathbf{B}_{\mathbf{fem}} d\Omega \right\} \mathbf{u} + \frac{1}{2}\mathbf{a}^{\mathbf{T}} \left\{ \int_{\Omega} \mathbf{B}_{\mathbf{enr}}^{\mathbf{T}} \mathbf{D}\mathbf{B}_{\mathbf{enr}} d\Omega \right\} \mathbf{a} \tag{20}$$

Let

$$\begin{aligned} \mathbf{K}_{\mathbf{uu}} &= \int_{\Omega} \mathbf{B}_{\mathbf{fem}}^{\mathbf{T}} \mathbf{D}\mathbf{B}_{\mathbf{fem}} d\Omega \\ \mathbf{K}_{\mathbf{ua}} &= \int_{\Omega} \mathbf{B}_{\mathbf{fem}}^{\mathbf{T}} \mathbf{D}\mathbf{B}_{\mathbf{enr}} d\Omega \\ \mathbf{K}_{\mathbf{au}} &= \int_{\Omega} \mathbf{B}_{\mathbf{enr}}^{\mathbf{T}} \mathbf{D}\mathbf{B}_{\mathbf{fem}} d\Omega \\ \mathbf{K}_{\mathbf{aa}} &= \int_{\Omega} \mathbf{B}_{\mathbf{enr}}^{\mathbf{T}} \mathbf{D}\mathbf{B}_{\mathbf{enr}} d\Omega \end{aligned} \tag{21}$$

Therefore

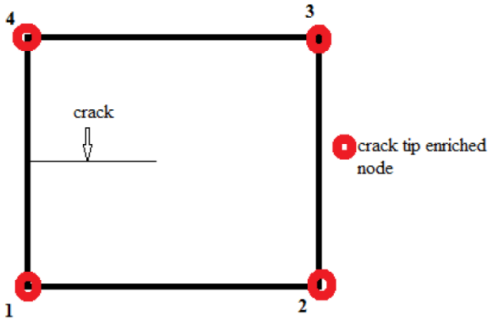

Fig. 5 Fully crack tip enriched element

$$U = \frac{1}{2}\left(\mathbf{u}^T\mathbf{K}_{uu}\mathbf{u} + \mathbf{u}^T\mathbf{K}_{ua}\mathbf{a} + \mathbf{a}^T\mathbf{K}_{au}\mathbf{u} + \mathbf{a}^T\mathbf{K}_{aa}\mathbf{a}\right) \tag{22}$$

Writing in matrix form

$$U = \frac{1}{2}\begin{bmatrix}\mathbf{u}^T & \mathbf{a}^T\end{bmatrix}\begin{bmatrix}\mathbf{K}_{uu} & \mathbf{K}_{ua}\\ \mathbf{K}_{au} & \mathbf{K}_{aa}\end{bmatrix}\begin{bmatrix}\mathbf{u}\\ \mathbf{a}\end{bmatrix} \tag{23}$$

Hence element stiffness matrix is given by

$$\mathbf{K}_e = \begin{bmatrix}\mathbf{K}_{uu} & \mathbf{K}_{ua}\\ \mathbf{K}_{au} & \mathbf{K}_{aa}\end{bmatrix} \tag{24}$$

Size of element stiffness matrix of four node bilinear element whose element nodes are completely enriched with Heaviside enriched nodes is 16×16

The element stiffness matrix for the crack tip element as shown in Fig. 5 is derived as follows

The displacement field within the element is given as

$$\begin{Bmatrix}u\\ v\end{Bmatrix} = \begin{bmatrix}\mathbf{N}_{fe} & \mathbf{N}_{en}^1 & \mathbf{N}_{en}^2 & \mathbf{N}_{en}^3 & \mathbf{N}_{en}^4\end{bmatrix}\begin{Bmatrix}\mathbf{u}\\ \mathbf{b}_1\\ \mathbf{b}_2\\ \mathbf{b}_3\\ \mathbf{b}_4\end{Bmatrix} \tag{25}$$

$$\mathbf{N}_{fe} = \begin{bmatrix}N_1 & 0 & N_2 & 0 & N_3 & 0 & N_4 & 0\\ 0 & N_1 & 0 & N_2 & 0 & N_3 & 0 & N_4\end{bmatrix} \tag{26}$$

$$\mathbf{N}_{en}^i = \begin{bmatrix}N_iF_1 & 0 & N_iF_2 & 0 & N_iF_3 & 0 & N_iF_4 & 0\\ 0 & N_iF_1 & 0 & N_iF_2 & 0 & N_iF_3 & 0 & N_iF_4\end{bmatrix} \qquad \forall i = 1,2,3,4 \tag{27}$$

$$\mathbf{u} = \{u_i\ v_i\}^T \quad \mathbf{b}_i = \{b_i^1\ c_i^1\ b_i^2\ c_i^2\ b_i^3\ c_i^3\ b_i^4\ c_i^4\}^T \tag{28}$$

Here *i* is the node number and strain displacement relation is given as

$$\{\boldsymbol{\varepsilon}\} = \begin{bmatrix} \mathbf{B_{fe}} & \mathbf{B_{en}^1} & \mathbf{B_{en}^2} & \mathbf{B_{en}^3} & \mathbf{B_{en}^4} \end{bmatrix} \begin{Bmatrix} \mathbf{u} \\ \mathbf{b_1} \\ \mathbf{b_2} \\ \mathbf{b_3} \\ \mathbf{b_4} \end{Bmatrix} \tag{29}$$

$$\mathbf{B_{fe}} = \begin{bmatrix} \frac{\partial N_1}{\partial x} & 0 & \frac{\partial N_2}{\partial x} & 0 & \frac{\partial N_3}{\partial x} & 0 & \frac{\partial N_4}{\partial x} & 0 \\ 0 & \frac{\partial N_1}{\partial y} & 0 & \frac{\partial N_2}{\partial y} & 0 & \frac{\partial N_3}{\partial y} & 0 & \frac{\partial N_4}{\partial y} \\ \frac{\partial N_1}{\partial y} & \frac{\partial N_1}{\partial x} & \frac{\partial N_2}{\partial y} & \frac{\partial N_2}{\partial x} & \frac{\partial N_3}{\partial y} & \frac{\partial N_3}{\partial x} & \frac{\partial N_4}{\partial y} & \frac{\partial N_4}{\partial x} \end{bmatrix} \tag{30}$$

$$\mathbf{B_{en}^i} = \begin{bmatrix} (N_i F_1)_{,x} & 0 & (N_i F_2)_{,x} & 0 & (N_i F_3)_{,x} & 0 & (N_i F_4)_{,x} & 0 \\ 0 & (N_i F_1)_{,y} & 0 & (N_i F_2)_{,y} & 0 & (N_i F_3)_{,y} & 0 & (N_i F_4)_{,y} \\ (N_i F_1)_{,y} & (N_i F_1)_{,x} & (N_i F_2)_{,y} & (N_i F_2)_{,x} & (N_i F_3)_{,y} & (N_i F_3)_{,x} & (N_i F_4)_{,y} & (N_i F_4)_{,x} \end{bmatrix}$$

$$\forall i = 1,2,3,4 \tag{31}$$

Therefore strain displacement matrix for the crack tip element is given as

$$\mathbf{B} = \begin{bmatrix} \mathbf{B_{fe}} & \mathbf{B_{en}^1} & \mathbf{B_{en}^2} & \mathbf{B_{en}^3} & \mathbf{B_{en}^4} \end{bmatrix} \tag{32}$$

Therefore element stiffness matrix of crack tip element is given as

$$\mathbf{K} = \int_{\Omega} \mathbf{B}^{\mathbf{T}} \mathbf{D} \mathbf{B} d\Omega \tag{33}$$

$$\mathbf{K} = \begin{bmatrix} \int_{\Omega} \mathbf{B_{fe}^T D B_{fe}} d\Omega & \int_{\Omega} \mathbf{B_{fe}^T D B_{en}^1} d\Omega & \int_{\Omega} \mathbf{B_{fe}^T D B_{en}^2} d\Omega & \int_{\Omega} \mathbf{B_{fe}^T D B_{en}^3} d\Omega & \int_{\Omega} \mathbf{B_{fe}^T D B_{en}^4} d\Omega \\ \int_{\Omega} \mathbf{B_{en}^{1T} D B_{fe}} d\Omega & \int_{\Omega} \mathbf{B_{en}^{1T} D B_{en}^1} d\Omega & \int_{\Omega} \mathbf{B_{en}^{1T} D B_{en}^2} d\Omega & \int_{\Omega} \mathbf{B_{en}^{1T} D B_{en}^3} d\Omega & \int_{\Omega} \mathbf{B_{en}^{1T} D B_{en}^4} d\Omega \\ \int_{\Omega} \mathbf{B_{en}^{2T} D B_{fe}} d\Omega & \int_{\Omega} \mathbf{B_{en}^{2T} D B_{en}^1} d\Omega & \int_{\Omega} \mathbf{B_{en}^{2T} D B_{en}^2} d\Omega & \int_{\Omega} \mathbf{B_{en}^{2T} D B_{en}^3} d\Omega & \int_{\Omega} \mathbf{B_{en}^{2T} D B_{en}^4} d\Omega \\ \int_{\Omega} \mathbf{B_{en}^{3T} D B_{fe}} d\Omega & \int_{\Omega} \mathbf{B_{en}^{3T} D B_{en}^1} d\Omega & \int_{\Omega} \mathbf{B_{en}^{3T} D B_{en}^2} d\Omega & \int_{\Omega} \mathbf{B_{en}^{3T} D B_{en}^3} d\Omega & \int_{\Omega} \mathbf{B_{en}^{3T} D B_{en}^4} d\Omega \\ \int_{\Omega} \mathbf{B_{en}^{4T} D B_{fe}} d\Omega & \int_{\Omega} \mathbf{B_{en}^{4T} D B_{en}^1} d\Omega & \int_{\Omega} \mathbf{B_{en}^{4T} D B_{en}^2} d\Omega & \int_{\Omega} \mathbf{B_{en}^{4T} D B_{en}^3} d\Omega & \int_{\Omega} \mathbf{B_{en}^{4T} D B_{en}^4} d\Omega \end{bmatrix} \tag{34}$$

For crack tip enriched element stiffness matrix of Eq. (34), size is 40x40 (for four node element)

Now we can generalise the formulation for any type of element. In this paper four node bi linear element has been used to model the plate. Hence the generalized element stiffness matrix formulation in XFEM for four node bilinear element is given as follows

The displacement field within the four node bi-linear element in the context of XFEM is given as

$$\mathbf{u^h(x)} = \begin{bmatrix} \mathbf{N^{fem}} & \mathbf{N^a} & \mathbf{N^b} \end{bmatrix} \begin{Bmatrix} \mathbf{u} \\ \mathbf{a} \\ \mathbf{b} \end{Bmatrix} \tag{35}$$

where, N^{fem} finite element shape functions, N^a and N^b shape functions modified due to enrichment with heaviside enrichment functions and crack tip enrichment function respectively

$$\mathbf{u^h(x)} = \begin{Bmatrix} u \\ v \end{Bmatrix}, \mathbf{N^{fem}} = \begin{bmatrix} N_1 & 0 & N_2 & 0 & N_3 & 0 & N_4 & 0 \\ 0 & N_1 & 0 & N_2 & 0 & N_3 & 0 & N_4 \end{bmatrix} \tag{36}$$

$$\mathbf{N^a} = \begin{bmatrix} \mathbf{N_1^a} & \mathbf{N_2^a} .... \mathbf{N_P^a} \end{bmatrix} \text{such that } \mathbf{N_P^a} = \begin{bmatrix} N_P H & 0 \\ 0 & N_P H \end{bmatrix} \tag{37}$$

$$\mathbf{N^b} = \begin{bmatrix} \mathbf{N_1^b} & \mathbf{N_2^b} .... \mathbf{N_Q^b} \end{bmatrix}, \mathbf{N_Q^b} = \begin{bmatrix} N_Q F_1 & 0 & N_Q F_2 & 0 & N_Q F_3 & 0 & N_Q F_4 & 0 \\ 0 & N_Q F_1 & 0 & N_Q F_2 & 0 & N_Q F_3 & 0 & N_Q F_4 \end{bmatrix} \tag{38}$$

$$\mathbf{u} = \{u_1, v_1, u_2, v_2, u_3, v_3, u_4, v_4\}^T \text{ and } \mathbf{a} = \{\mathbf{a_1}, \mathbf{a_2}, ..., \mathbf{a_p}\}^T \text{ where } \mathbf{a_P} = \{a_P, b_P\} \tag{39}$$

$$\mathbf{b} = \{\mathbf{b_1}, \mathbf{b_2}, ..., \mathbf{b_Q}\} \text{where } \mathbf{b_Q} = \{b_Q^1, c_Q^1, b_Q^2, c_Q^2, b_Q^3, c_Q^3, b_Q^4, c_Q^4\} \tag{40}$$

Here *P*, *Q* represents the number of nodes in bi-linear elements enriched with heaviside enrichment function and crack tip enrichment functions respectively such that, depending on the position of the crack, $1 \le P, Q \le 4$.

Now, the strain displacement relation is obtained as

$$\mathbf{B_u} = \begin{bmatrix} N_{1,x} & 0 & N_{2,x} & 0 & N_{3,x} & 0 & N_{4,x} & 0 \\ 0 & N_{1,y} & 0 & N_{2,y} & 0 & N_{3,y} & 0 & N_{4,y} \\ N_{1,y} & N_{1,x} & N_{2,y} & N_{2,x} & N_{3,y} & N_{3,x} & N_{4,y} & N_{4,x} \end{bmatrix} \tag{41}$$

$$\mathbf{B_a} = \begin{bmatrix} \mathbf{B_1^a} & \mathbf{B_2^a} ... \mathbf{B_P^a} \end{bmatrix} \text{where } \mathbf{B_P^a} = \begin{bmatrix} (N_P H)_{,x} & 0 \\ 0 & (N_P H)_{,y} \\ (N_P H)_{,y} & (N_P H)_{,y} \end{bmatrix} \tag{42}$$

$$\mathbf{B_b} = \begin{bmatrix} \mathbf{B_1^b} & \mathbf{B_2^b} ... \mathbf{B_Q^b} \end{bmatrix} \tag{43}$$

$$\mathbf{B_Q^b} = \begin{bmatrix} (N_Q F_1)_{,x} & 0 & (N_Q F_1)_{,x} & 0 & (N_Q F_1)_{,x} & 0 & (N_Q F_1)_{,x} & 0 \\ 0 & (N_Q F_1)_{,x} & 0 & (N_Q F_1)_{,x} & 0 & (N_Q F_1)_{,x} & 0 & (N_Q F_1)_{,x} \\ (N_Q F_1)_{,x} & (N_Q F_1)_{,x} & (N_Q F_1)_{,x} & (N_Q F_1)_{,x} & (N_Q F_1)_{,x} & (N_Q F_1)_{,x} & (N_Q F_1)_{,x} & (N_Q F_1)_{,x} \end{bmatrix} \tag{44}$$

Therefore element stiffness matrix is given by

$$\mathbf{K} = \int_{\Omega} \mathbf{B^T D B} d\Omega \tag{45}$$

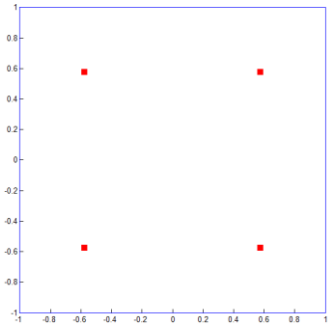

(a) Classical finite element

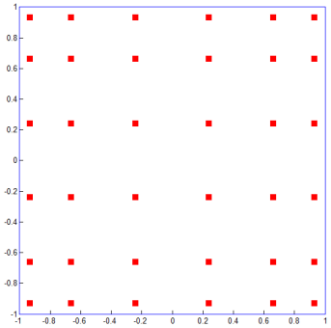

(b) Partially enriched element

Fig. 6 Gauss quadrature integration scheme for (a) classical finite element and (b) partially enriched element

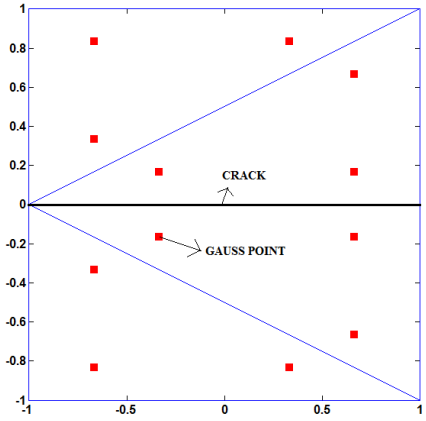

(a) Element fully cut by the crack

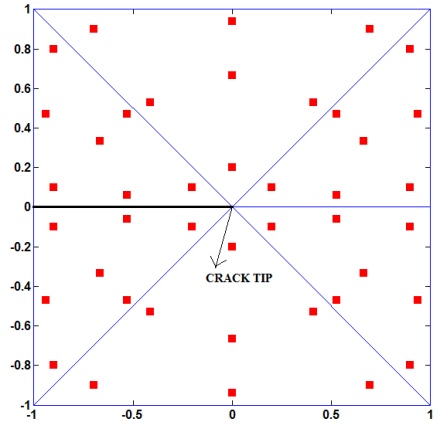

(b) Element containing the crack tip

Fig. 7 Element subdivision strategy for numerical integration for elements cut by the crack

$$\mathbf{B} = \begin{bmatrix} \mathbf{B}_u & \mathbf{B}_a & \mathbf{B}_b \end{bmatrix} \tag{46}$$

Substituting Eq. (46) in Eq. (45), element stiffness matrix in XFEM is obtained as

$$\mathbf{K} = \begin{bmatrix} \mathbf{K}_{uu} & \mathbf{K}_{ua} & \mathbf{K}_{ub} \\ \mathbf{K}_{au} & \mathbf{K}_{aa} & \mathbf{K}_{ab} \\ \mathbf{K}_{bu} & \mathbf{K}_{ba} & \mathbf{K}_{bb} \end{bmatrix} = \begin{bmatrix} \int_\Omega \mathbf{B}_u^T \mathbf{D} \mathbf{B}_u d\Omega & \int_\Omega \mathbf{B}_u^T \mathbf{D} \mathbf{B}_a d\Omega & \int_\Omega \mathbf{B}_u^T \mathbf{D} \mathbf{B}_a d\Omega \\ \int_\Omega \mathbf{B}_a^T \mathbf{D} \mathbf{B}_u d\Omega & \int_\Omega \mathbf{B}_a^T \mathbf{D} \mathbf{B}_a d\Omega & \int_\Omega \mathbf{B}_a^T \mathbf{D} \mathbf{B}_b d\Omega \\ \int_\Omega \mathbf{B}_b^T \mathbf{D} \mathbf{B}_u d\Omega & \int_\Omega \mathbf{B}_b^T \mathbf{D} \mathbf{B}_a d\Omega & \int_\Omega \mathbf{B}_b^T \mathbf{D} \mathbf{B}_b d\Omega \end{bmatrix} \tag{47}$$

2.2 Numerical integration

Evaluation of element stiffness matrix requires numerical integration. As there are different types of elements, depending on the nodal enrichment, a single standard gauss quadrature scheme

cannot be used for all types of elements. In this paper, four node bilinear elements are used and following integration scheme is used for different elements.

For elements cut by the crack, element subdivision is done along the crack segment (Moes *et al*. 1999) such that each sub division is a triangle and new set of gauss points are derived for each triangle as shown in the Fig. 7

For classical finite element, standard 2×2 gauss integration scheme is used and for partially enriched element a higher order 6×6 gauss quadrature scheme is used as shown in Fig. 6

2.3 Finite element modelling of stiffeners

As the stiffeners are placed concentric and the applied loading is tensile in nature, one can model the stiffeners using truss elements. It is assumed that stiffeners are continuous and are connected to the plate along the nodes of the plate element modelled as bilinear element. For example consider a square plate of side L modelled using four bilinear elements of side l and an edge stiffener using two node truss element as shown in Fig. 8.

Assuming that the Young's modulus of stiffener and Young's modulus of panel is same and denoted it as E and area of cross section of each stiffener as A. The length of truss element is same as side of bilinear element. Thus element stiffness matrix of truss element is given as

$$\mathrm{k} = \frac{\mathrm{AE}}{\mathrm{l}}\begin{bmatrix} 1 & -1 \\ -1 & 1 \end{bmatrix} \tag{48}$$

The global stiffness matrix of panel modelled using four node bilinear element be K_p. Size of K_p depends upon the location and position of the crack in the panel. The assembled stiffness matrix of stiffeners modelled as truss elements can be obtained as

$$K_{t1} = \frac{AE}{l}\begin{matrix} \\ 2 \\ 8 \\ 14 \end{matrix}\begin{matrix} \begin{bmatrix} 1 & -1 & 0 \\ -1 & 2 & -1 \\ 0 & -1 & 1 \end{bmatrix} \end{matrix}\begin{matrix} 2 & 8 & 14 \end{matrix} \qquad K_{t2} = \frac{AE}{l}\begin{matrix} \\ 6 \\ 12 \\ 18 \end{matrix}\begin{matrix} \begin{bmatrix} 1 & -1 & 0 \\ -1 & 2 & -1 \\ 0 & -1 & 1 \end{bmatrix} \end{matrix}\begin{matrix} 6 & 12 & 18 \end{matrix} \tag{49}$$

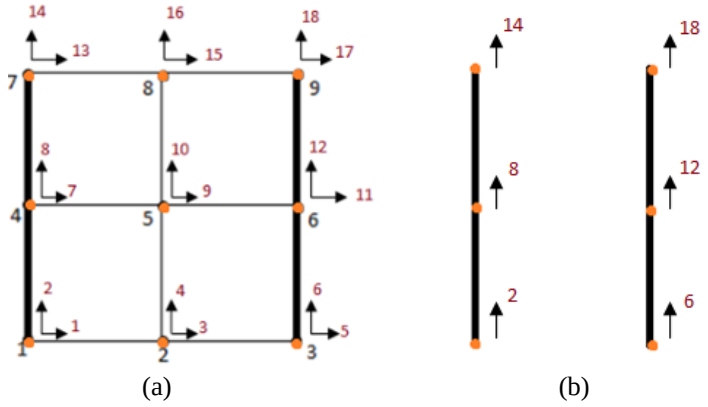

(a) (b)

Fig. 8 (a) Finite element model of plate using four node bilinear element (b) Finite element model of stiffeners using two node truss element

where K_{t1} and K_{t2} are the assembled global stiffness matrices of stiffener 1 and stiffener 2 respectively each of size equal to K_p. Note that the matrices shown in Eq. (49) are only sub matrices and the values in other locations of matrices K_{t1} and K_{t2} are zero

Thus the final stiffness matrix of panel and stiffener is

$$K = K_p + K_{t1} + K_{t2} \tag{50}$$

Similar lines the final stiffness matrix of panel and stiffener for various mesh discretizations can be formulated.

2.4 Level set method

Level set method (Stolarska *et al*. 2001) has been implemented in this paper to model the crack in XFEM framework. The main advantage of level set method is that it offers a convenient way to identify the elements which are cut by the crack, identify the nodes to be enriched. In level set method crack is considered to be a one dimensional manifold in the two dimensional domain and crack is represented as zero of the level set function. Level set values are taken positive on one side of the interface and negative on the other side. Signed distance function is used as level set function and is given as

$$\phi(\mathbf{x}) = \pm \min \left\| \mathbf{x} - \mathbf{x}^* \right\|, \mathbf{x}^* \in \Gamma_c \forall \mathbf{x} \in \Omega \tag{51}$$

where, Ω is the problem domain and Γ_c is the crack. The sign is different on the two sides of the interface and can be determined from sign($\mathbf{n}\cdot(\mathbf{x}-\mathbf{x}^*)$) with $\mathbf{x}^*$ being the closest point on the interface to $\mathbf{x}$. In crack modelling we require two level set functions to represent the crack and crack tips as shown in Fig. 9.

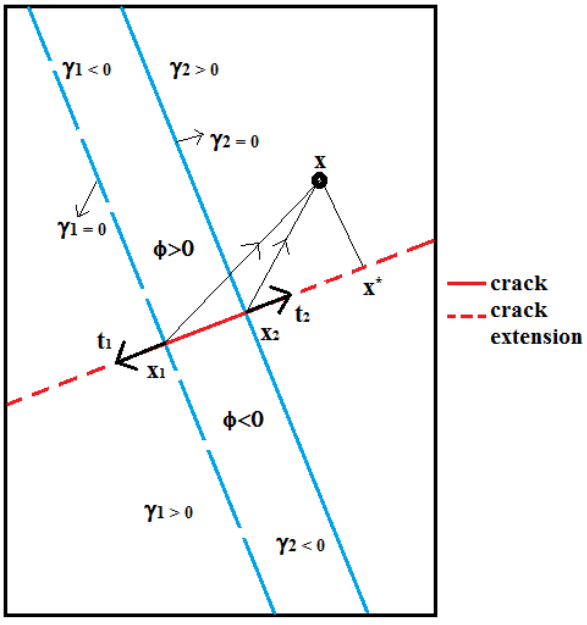

Fig. 9 Level set representation of crack

End point of the crack is represented as the intersection of zero level curve with the orthogonal zero level set $\gamma_i(x)$, where i is the number of tips on a given crack. The values of the level set functions are stored only at the nodes. The functions are interpolated over the mesh by the same shape functions as the displacement. Thus

$$\gamma_i(\mathbf{x}) = \sum_{j \in J} \gamma_{ij} N_j(\mathbf{x}) \quad \phi(x) = \sum_{j \in J} \phi_j N_j(\mathbf{x}) \tag{52}$$

Level set function that represented the crack tip are initially represented as

$$\gamma_i(\mathbf{x}) = (\mathbf{x} - \mathbf{x_i}).\mathbf{t_i} \tag{53}$$

where $\mathbf{t_i}$ is a unit vector tangent to the crack at its tip and $\mathbf{x}_i$ is the location of the ith crack tip. In Eq. (50), the planar function γ_i have a zero level set which is orthogonal to at the crack tip. The initial level set functions, φ and γ_i, and the representation of the crack are shown in Fig. 8. If there are two crack tips then crack tip level set function is taken as maximum of $\gamma_i(\mathbf{x})$. Thus crack is defined as the set

$$\text{crack} = \{\mathbf{x} : \phi(\mathbf{x}) = 0 \ \text{ and } \ \gamma_i(\mathbf{x}) \le 0\} \tag{54}$$

Since only the evolution of a one dimensional curve is considered, the updating of level sets on the entire two dimensional domain is not considered. Thus, the level set representation is confined to a narrow band of elements around the crack and level set values need to be updated as the crack propagates.

3. Stress intensity factor computation

The domain form of interaction integral for two equilibrium states has been used to compute the mixed mode stress intensity factor (Yau *et al.* 1980, Moes *et al.* 1999) which is given as

$$I^{(1,2)} = \int_A \left[\sigma_{ij}^{(1)} \frac{\partial u_i^{(2)}}{\partial x_1} + \sigma_{ij}^{(2)} \frac{\partial u_i^{(1)}}{\partial x_1} - W^{(1,2)} \delta_{1j} \right] \frac{\partial q}{\partial x_j} \tag{55}$$

where superscript (1) represents the equilibrium state corresponding to the XFEM analysis and superscript (2) represents the auxiliary equilibrium state corresponding to Westergaard's stress analysis. $W^{(1,2)}$ is the interaction strain energy density given as

$$W^{(1,2)} = \sigma_{ij}^{(1)} \varepsilon_{ij}^{(2)} = \sigma_{ij}^{(2)} \varepsilon_{ij}^{(1)} \tag{56}$$

For the numerical evaluation of the above integral, the domain A is set from the collection of elements about the crack tip as shown in Fig. 10. The characteristic length of an element touched by the crack tip is calculated as the square root of the element area and denoted as h_{local}. The domain A is then set to be all elements which have a node within a ball of radius r_d (in this paper r_d is taken as three times of h_{local}) about the crack tip as shown in Fig 10 and q is the smoothing function which takes the value 1 at the nodes within the ball radius r_d and zero on the outer contour and intermediate values are interpolated using shape functions. Once the interaction integral is computed, then mixed mode stress intensity factor is computed as

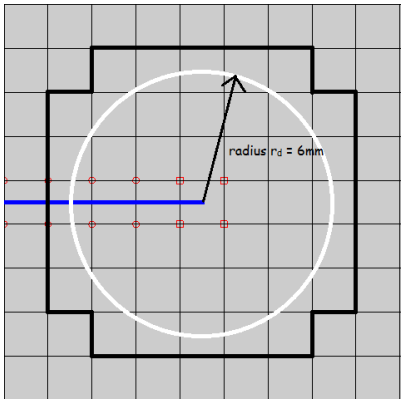

Fig. 10 Domain for the computation of interaction integral

$$K_I^{(1)} = \frac{I^{(1,2a)}}{2\alpha} \qquad K_{II}^{(1)} = \frac{I^{(1,2b)}}{2\alpha} \tag{57}$$

where 2*a*, 2*b* corresponds to near tip auxiliary state obtained from Westergaard's analysis for pure Mode I and Mode II respectively. α is given as $(1-\upsilon^2)/E$ for plane strain and $1/E$ for plane stress. In this paper domain for computing SIF is taken as r_d which is equal to three times the square root of area of finite element.

4. Direction and magnitude of crack growth

To model the fatigue crack growth, first the discrete set of equilibrium equations Ku=f have been solved from XFEM and the results have been used to compute the interaction integral given in Eq. (56) and stress intensity factors from Eq. (57). The amount of crack growth depends upon the crack growth law. The maximum hoop stress ($\sigma_{\theta\theta}$) criteria (Erdogan and Sih 1963) has been used to predict the direction of crack propagation i.e., crack shall propagate in the direction where $\sigma_{\theta\theta}$ is maximum which is given for $-\pi<\theta_c<\pi$ as

$$\theta_c = 2\arctan\frac{1}{4}\left(\frac{K_I}{K_{II}} \pm \sqrt{\left(\frac{K_I}{K_{II}}\right)^2 + 8}\right) \tag{58}$$

The magnitude of incremental crack is determined from Paris's crack growth law (Paris *et al*. 1961) defined as

$$\frac{da}{dN} = C(\Delta K)^m \tag{59}$$

where *C* and *m* are Paris law constants defined for a material and ΔK is the equivalent mixed mode stress intensity factor range given by Tanaka (1974) as

$$\Delta K = \sqrt[4]{K_I^4 + 8K_{II}^4} \tag{60}$$

Magnitude of incremental crack Δa is computed for a number of fatigue cycles ΔN. In this paper for each iteration ΔN is taken as 1000 cycles and for each 1000 cycles Δa is computed using Paris crack growth law equation given as

$$\Delta a = C(\Delta K)^m \Delta N \tag{61}$$

Once Δa is computed, initial crack geometry is updated and new set of level set values are updated by computing the new set of level set values at the nodes.

Flow chart of XFEM code is

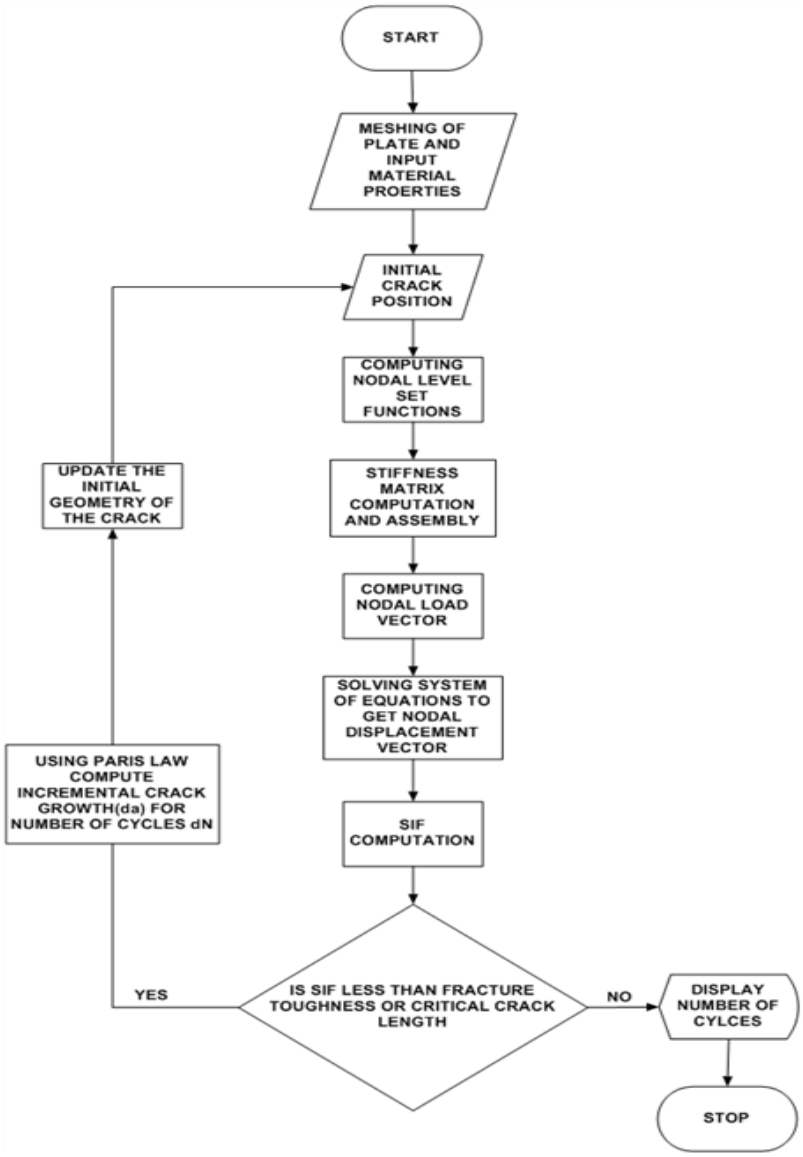

Fig. 11 Flow chart of XFEM code

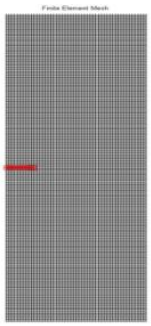

Fig. 12 (a) XFEM model of plate with edge crack

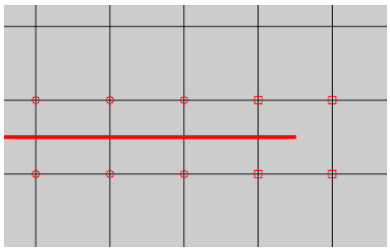

Fig. 12 (b) zoomed view of mesh with enrichment near the vicinity of the crack

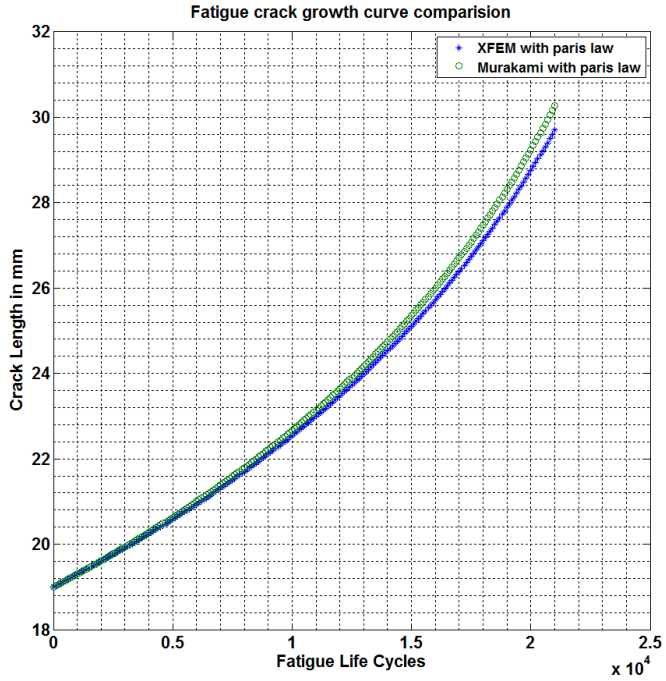

Fig. 13 Fatigue crack growth curve comparison between XFEM with Paris law and Murakami handbook with Paris law(Reference curve)

5. Numerical examples

The implementation of XFEM has been verified/applied for fatigue and fracture analysis of stiffened and unstiffened 350WT steel panels. In all numerical examples following properties of the panel have been used

- Size of panel $2h \times 2b = 310 \times 100$ mm
- Material is homogeneous, isotropic and made up of 350WT Steel
- Young's modulus$=2\times10^5$ N/mm^2
- Poisson's ratio$=0.3$

- Panel is modelled with four node bilinear element of size 2 mm×2 mm
- Stiffener is modelled with two node truss element
- Plane strain linear elastic fracture mechanics assumption
- Paris crack growth law constants $C=1.02\times10^{-11}$, $m=2.94$
- Fracture toughness $K_{IC}=50$ MPa√m

5.1 Plate with centred edge crack

An unstiffened plate of centred edge crack of length 19 mm is subjected to a constant amplitude fatigue loading with $\sigma_{max}=100$ N/mm^2 and $\sigma_{min}=0$ have been used. Fig. 12 shows the XFEM model used for the analysis and the analysis is continued till the stress intensity factor reaching the fracture toughness of the material. Results obtained are shown in Fig. 13

From Fig. 13 the XFEM results with Paris crack growth law curve are in good agreement with that of Murakami handbook (Murakami 1986) with Paris crack growth law curve. For 21000 number of cycles of loading, XFEM has predicted a crack length of 29.701 mm and Murakami (Murakami 1986) with Paris law predicted a crack length of 30.270 mm.

5.2 Centre cracked plate with edge stiffeners

Stress intensity factor has been computed for 350 WT edge stiffened centre cracked panel subjected to uniaxial tensile stress of $\sigma=100$ N/mm^2 for various stiffener areas (s=ratio of area of stiffener to half width of plate) and various crack width to plate width ratios (a/b) using XFEM analysis and the results are compared with the Rooke and Cartwright handbook (Rooke *et al*. 1976) in which the results are available only for the edge stiffeners. The results obtained are shown in the Tables 1 to 6 which shows the comparison of SIF values between XFEM analysis and Rook, Cartwright hand book.

Table 1 a/b= 0.1 and $K_0=\sigma\sqrt{(\pi a)}=12.533$ MPa√m

Area of Stiffener mm^2	$s=A/b$	K_{IROOKE} MPa√m	K_{IXFEM} MPa√m
0	0	12.658	13.079
5	0.1	11.4051	11.9716
10	0.2	10.5277	11.045
17.5	0.35	9.211	9.919
25	0.5	8.397	9.0254
37.5	0.75	6.893	7.8902

Table 2 a/b=0.2 and $K_0=\sigma\sqrt{(\pi a)}=17.724$ MPa√m

Area of Stiffener mm^2	$s=A/b$	K_{IROOKE} MPa√m	K_{IXFEM} MPa√m
0	0	18.362	18.587
5	0.1	16.483	16.987
10	0.2	14.976	15.654
17.5	0.35	13.381	14.036
25	0.5	11.96	12.756
37.5	0.75	10.235	11.133

Table 3 a/b=0.3 and $K_0=\sigma\sqrt{(\pi a)}$=21.708 MPa√m

Area of Stiffener mm^2	$s=A/b$	K_{IROOKE} MPa√m	K_{IXFEM} MPa√m
0	0	23.01	23.98
5	0.1	20.405	21.803
10	0.2	18.668	20.01
17.5	0.35	16.927	17.85
25	0.5	14.761	16.16
37.5	0.75	12.5906	14.03

Table 4 a/b=0.4 and $K_0=\sigma\sqrt{(\pi a)}$=25.066 MPa√m

Area of Stiffener mm^2	$s=A/b$	K_{IROOKE} MPa√m	K_{IXFEM} MPa√m
0	0	27.62	28.348
5	0.1	24.815	25.635
10	0.2	22.496	23.434
17.5	0.35	19.614	20.81
25	0.5	17.5462	18.77
37.5	0.75	14.788	16.22

Table 5 a/b=0.5 and $K_0=\sigma\sqrt{(\pi a)}$=28.024 MPa√m

Area of Stiffener mm^2	$s=A/b$	K_{IROOKE} MPa√m	K_{IXFEM} MPa√m
0	0	33.236	34.471
5	0.1	29.705	30.759
10	0.2	26.342	27.841
17.5	0.35	22.7	24.448
25	0.5	20.177	21.86
37.5	0.75	16.8144	18.686

Table 6 a/b=0.6 and $K_0=\sigma\sqrt{(\pi a)}$=30.7 MPa√m

Area of Stiffener mm^2	$s=A/b$	K_{IROOKE} MPa√m	K_{IXFEM} MPa√m
0	0	39.91	39.97
5	0.1	34.506	35.24
10	0.2	30.546	31.613
17.5	0.35	25.849	27.481
25	0.5	22.718	24.383
37.5	0.75	18.88	20.643

Using the results of Tables 1 to 6, polynomial curve fitting has been done in MATLAB and the best fit results are shown in Fig. 14 whose x axis is a/b and y axis is K_I/K_0. From Tables 1 to 6 and Fig. 14 following observations can be drawn. 1. As the area of stiffener increases SIF values are decreasing. 2. The SIF results obtained from XFEM analysis are in good agreement with that of literature (Rooke *et al*. 1976) and 3. Always XFEM analysis is over predicting the SIF values when compared to SIF obtained from literature (Rooke *et al.* 1976).

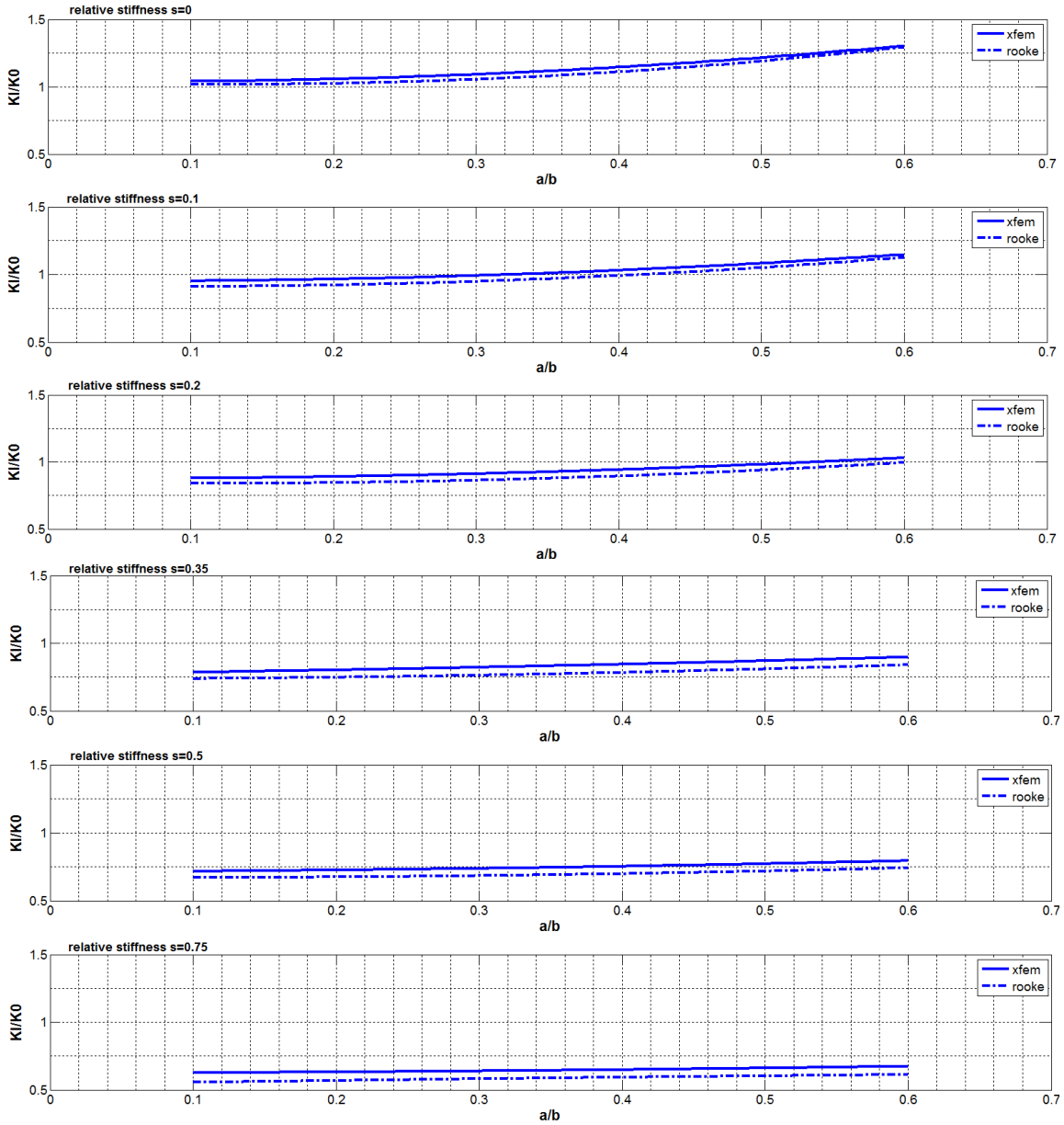

Fig. 14 Comparison of XFEM results with Rooke *et al*. (1976) for various values of s

5.3 Fatigue life estimation of centre cracked plate with edge stiffeners

In this section 350 WT steel stiffened plate with centre crack of 2a=20 mm whose properties and modelling are described in the beginning of this section is subjected to a constant amplitude fatigue tensile loading of σ_{max}=100 Mpa and σ_{min}=0 Mpa is analysed. The XFEM analysis has been carried out and fatigue life criteria has been set as crack length reaching the 60% of plate width i.e., fatigue life has been defined as the number of cycles required for a crack to grow up to 60% of

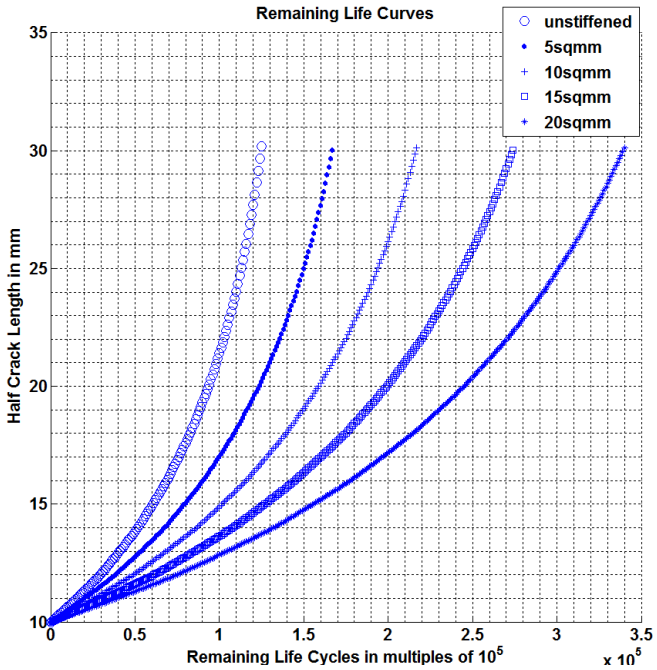

Fig. 15 Fatigue life curves for centre cracked panel of initial crack length of 2*a*=20 mm and edge stiffened with various areas of stiffeners

Table 7 Fatigue life and gain in life for edge stiffened centre crack panels using XFEM analysis

Area of Stiffener in mm^2	Predicted Fatigue life in number of cycles using XFEM analysis	Gain in fatigue life in percentage compared to unstiffened panel
0	125000	-
5	167000	33.6 %
10	217000	73.6 %
15	274000	119.2%
20	340000	172%

plate width. The results obtained are shown in Fig. 15 and Table 7.

From Fig. 15 and Table 7 it is clear that compared to unstiffened panels there is a considerable gain in the fatigue life when the panels are stiffened.

5.4 Damage tolerant curves generation for plate with a centre crack using XFEM

A 350WT steel plate of width (2b) 100 mm, height (2h) 310 mm with a centre crack is subjected to tensile fatigue loading as shown in Fig. 16(a) and Fig. 16(b). The objective is to predict the number of fatigue cycles required for given applied stress range for a plate with centre crack using XFEM and get the applied stress range versus number of fatigue cycles required to fail i.e., the damage tolerant curves. The failure criterion of the plate has been set as the crack length reaching 60% of plate width or fracture toughness of the plate whichever is earlier. The assumptions are given in the beginning of this section.

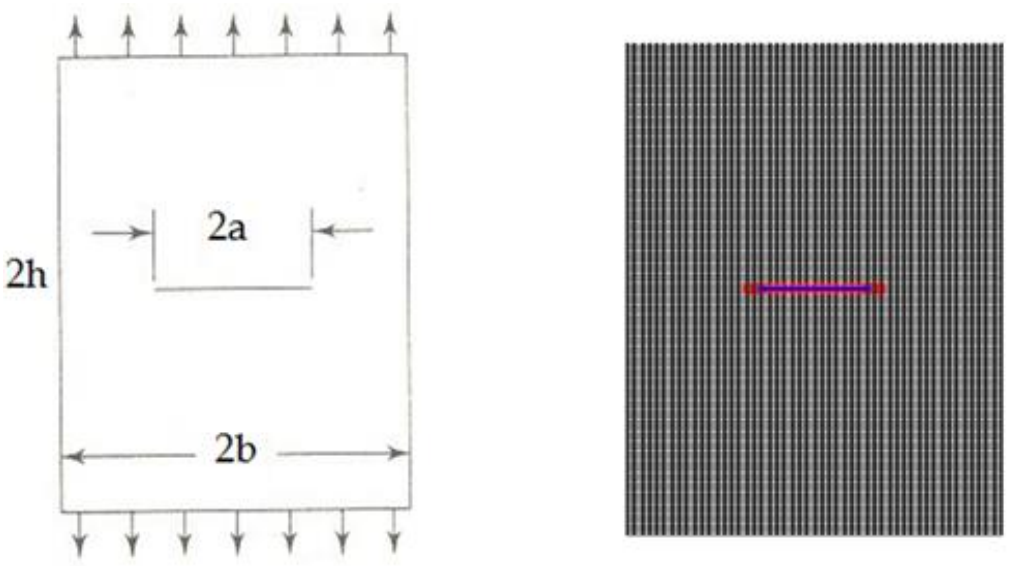

(a) (b)

Fig. 16 (a) Plate with centre crack subjected to tensile fatigue loading. (b) XFEM model of the plate with centre crack

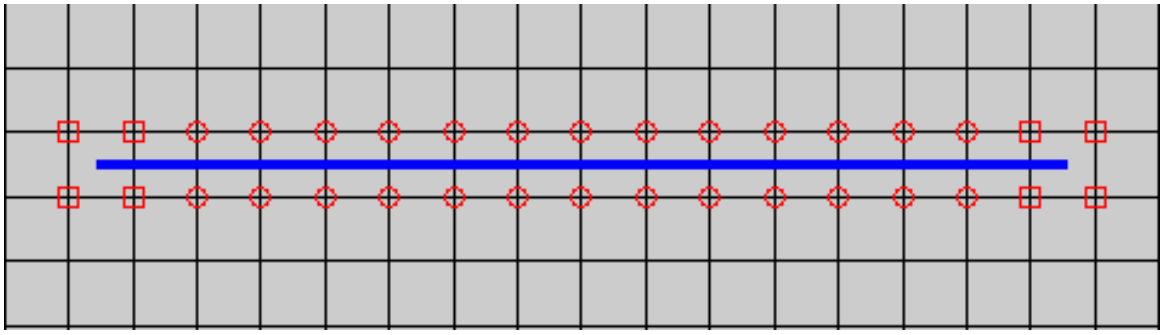

Fig. 17 Zoomed view of the mesh near the crack

Fig. 17 shows the zoomed view of the mesh near the crack. Circled nodes are enriched with heaviside enrichment function and squared nodes are enriched with crack tip enrichment function. The damage tolerant curves are shown in Fig. 18.

Stress range is varied from 200 MPa to 40 MPa for various initial crack length to plate width ratios (*a/b*) 0.1, 0.2 and 0.3. For each stress range XFEM analysis as described in previous sections and given in Flow chart of Fig. 8 is carried out to find the number of fatigue cycles required to fail. The results obtained are shown in Fig. 18, as applied stress range versus number of fatigue life cycles in the form of semi-log plot.

From the results shown in Fig. 18, as the external applied stress is decreasing number of fatigue life cycles taken by the component is increasing. This figure gives the quick idea about the number of cycles a crack of initial length to plate width ratio between 0.1 and 0.3 can take for applied stress range between 200 MPa and 40 Mpa.

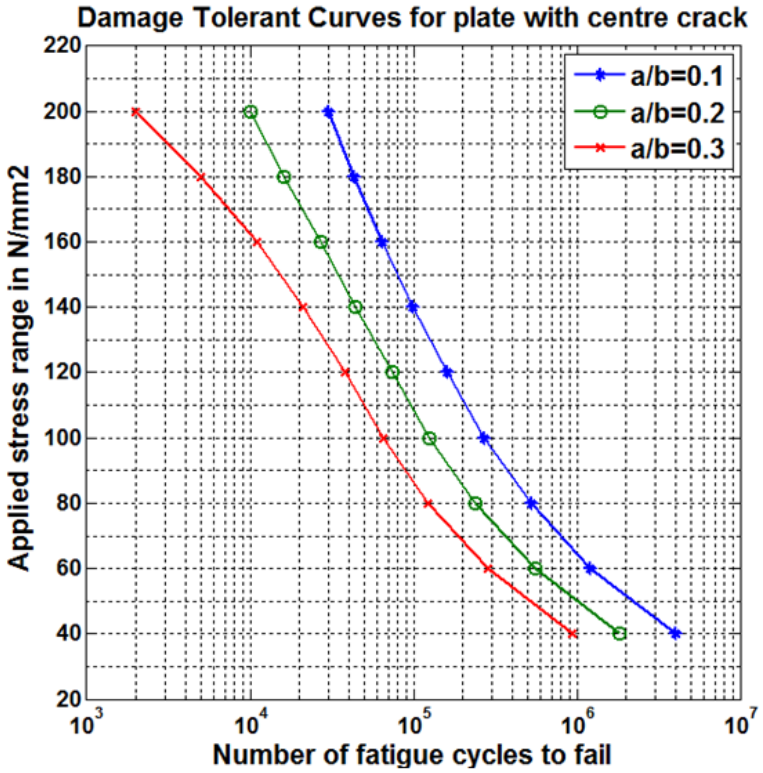

Fig. 18 Damage tolerant curves for plate with centre crack

6. Conclusions

An attempt has been made for the generation of damage tolerant curves and remaining life estimation of cracked unstiffened and concentric stiffened panels. XFEM formulations have been presented in detail and fracture analysis has been carried out for 350WT steel stiffened and unstiffened panels subjected to tensile loading. XFEM solutions are used to calculate the stress intensity factor using the domain form of interaction integral technique. Panel is modelled using four node bilinear isoparametric element and stiffener is modelled using truss element. Stress intensity factor obtained from XFEM solutions are compared with that of stress intensity factors available in handbooks and the SIFs obtained using XFEM analysis are in good agreement with that of SIFs obtained using handbooks. Further, the fatigue life analysis has been carried out on unstiffened panel with centre edge crack and edge stiffened panel with centre crack. Fatigue crack growth curves are obtained for various stiffener areas. It is observed that there is a considerable increase in fatigue life of stiffened panels when compared to unstiffened panels.

In order to generate damage tolerant curves, SIF computed from XFEM analysis is substituted in Paris's crack growth to compute the incremental crack growth (Δa) for a given number of fatigue cycles (ΔN) up to failure. The process is repeated for various applied stress ranges ($\Delta\sigma$) and corresponding to each $\Delta\sigma$ fatigue cycles to failure has been computed. This data has been used to generate curves known as damage tolerant curves which give information regarding given a plate with initial crack geometry and applied stress range, what would be the number of fatigue cycles

the cracked plate can take before undergoing failure. These curves give quick information regarding the fatigue life of a cracked structural component subjected to given constant amplitude tensile loading.

Acknowledgements

This paper is being published with the kind permission of The Director, CSIR SERC Chennai.

References

Belytschko, T. and Black, T. (1999), "Elastic crack growth in finite elements with minimal remeshing", *Int. J. Numer. Meth. Eng.*, **45**, 601-620.

Dexter, R.J., Pilarski, P.J. and Mahmoud, H.N. (2003), "Analysis of crack propagation in welded stiffened panels", *Int. J. Fatig.*, **25**, 1169-1174.

Dolbow, J., Moes, N. and Belytschko, T. (2000), "Discontinuous enrichment in finite elements with a partition of unity method", *Finite Elem. Anal. Des.*, **36**, 235-260.

Erdogan, F. and Sih, G.C. (1963), "On the crack extension in plates under plane loading and transverse shear", *J. Basic Eng.*, **85**, 519-527.

Jamal-Omidi, M., Falah, M. and Taherifar, D. (2014), "3-D fracture analysis of cracked aluminum plates repaired with single and double composite patches using XFEM", *Struct. Eng. Mech.*, **50**(4), 525-539.

Jiang, S.Y., Du, C.B. and Gu, C.S. (2014), "An investigation into the effects of voids, inclusions and minor cracks on major crack propagation by using XFEM", *Struct. Eng. Mech.*, **49**(5), 597-618.

Kocanda, D. and Jasztal, M. (2012), "Probabilistic predicting the fatigue crack growth under variable amplitude loading", *Int. J. Fatig.*, **39**, 68-74.

Mahmoud, H.N. and Dexter, R.J. (2005), "Propagation rate of large cracks in stiffened panels under tension loading", *Mar. Struct.*, **18**(3), 265-288.

Melenk, J.M. and Babuska, I. (1996), "The partition of unity finite element method: basic theory and applications", *Comput. Meth. Appl. Mech. Eng.*, **139**, 289-314.

Meng, Q. and Wang, Z. (2014), "Extenede finite element method for power law creep crack growth", *Eng. Fract. Mech.*, **127**, 148-160.

Moes, N., Dolbow, J. and Belytschko, T. (1999), "A finite element method for crack growth without remeshing", *Int. J. Numer. Meth. Eng.*, **46**, 131-150.

Murakami (1986), "Stress intensity factor handbook", Pergamon press.

Natarajan, S., Kerfriden, P., Roy Mahapatra, D. and Bordas, S.P.A. (2014), "Numerical analysis of the inclusion-crack interaction by the extended finite element method", *Int. J. Comput. Meth. Eng. Sci. Mech.*, **15**, 26-32.

Nechval, K.N., Nechval, N.A., Bausova, I., Skiltere, D. and Strelchonok, V.F. (2006), "Prediction of fatigue crack growth process via artificial neural network process", *Int. J. Comput.*, **5**(3), 21-32.

Paris, P., Gomez, M. and Anderson, W. (1961), "A rational analytic theory of fatigue", *Trend Eng.*, **13**, 9-14.

Pathak, H., Singh, A. and Vir Singh, I. (2013), "Fatigue crack growth simulations of 3-D problems using XFEM", *Int. J. Mech. Sci.*, **76**, 112-131.

Rama Chandra Murthy, A., Palani, G.S. and Iyer, N.R. (2007), "Remaining life prediction of cracked stiffened panels under constant and variable amplitude loading", *Int. J. Fatig.*, **29**(6), 1125-1139.

Rama Chandra Murthy, A., Palani, G.S. and Iyer, N.R. (2009a), "Damage tolerant evaluation of cracked stiffened panels subjected to fatigue loading", *Sadhana*, **37**(1), 171-186.

Rama Chandra Murthy, A., Palani, G.S. and Iyer, N.R. (2009b), "Residual strength evaluation of unstiffened and stiffened panels under fatigue loading", *SDHM*, **5**(3), 201-226.

Rasuo, B., Grbovic, A. and Petrasinovic, D. (2013), "Investigation of fatigue life of 2024-T3 aluminium spar using extended finite element method (XFEM) ", *SAE Int. J. Aerosp.*, **6**(2), 408-416.

Rooke, D.P. and Cartwright, D.J. (1976), *Compendium of Stress Intensity Factors*, Her Majesty's Stationary Office, London.

Sabelkin, V., Mall, S. and Avram, A.V. (2006), "Fatigue crack growth analysis of stiffened cracked panel repaired with bonded composite patch", *Eng. Fract. Mech.*, **73**, 1553-1567.

Sharma, K., Singh, I.V., Mishra, B.K. and Shedbale, A.S. (2014), "The effect of inhomogeneities on an edge crack: A numerical study using XFEM", *Int. J. Comput. Meth. Eng. Sci. Mech*., **14**, 505-523.

Singh, I.V., Mishra, B.K., Bhattacharya, S. and Patil, R.U. (2012), "The numerical simulation of fatigue crack growth using extended finite element method", *Int. J. Fatig.*, **36**, 109-119.

Stolarska, M., Chopp, D.L., Moes, N. and Belyschko, T. (2001), "Modelling crack growth by level sets in the extended finite element method", *Int. J. Numer. Meth. Eng*., **51**, 943-960.

Tanaka, K. (1974), "Fatigue crack propagation from a crack inclined to the cyclic tension axis", *Eng. Fract. Mech.*, **6**, 493-507.

Tong, P. and Pian, T.H. (1973), "On the convergence of the finite element method for problems with singularity", *Int. J. Solid. Struct.*, **9**, 313-321.

Yau, J., Wang, S. and Corten, H. (1980), "A mixed-mode crack analysis of isotropic solids using conservation laws of elasticity", *J. Appl. Mech.*, **47**, 335-341.

CC